



ISSN: 0975-833X

RESEARCH ARTICLE

MAGNETIC AND RADIATION ABSORPTION EFFECTS ON THERMOSOLUTAL CONVECTION IN A HORIZONTAL POROUS LAYER SUBJECT TO CROSS FLUXES OF HEAT AND MASS

*Amos, E. and Israel-Cookey, C.

Department of Mathematics and Computer Science, Rivers State University of Science and Technology, Port Harcourt, Nigeria

ARTICLE INFO

Article History:

Received 13th April, 2015
Received in revised form
28th May, 2015
Accepted 02nd June, 2015
Published online 31st July, 2015

Key words:

Natural convection, Radiation absorption,
Magnetic field, Porous medium,
Thermal Rayleigh number.

ABSTRACT

This study investigates the effect of electromagnetic field and radiation absorption on natural convection in a horizontal shallow porous cavity filled with an electrically conducting binary fluid. The vertical and horizontal walls of the cavity are subjected to cross fluxes of heat and mass. The Darcy model, Rosseland approximation for the radiative flux and the Boussinesq approximation for density variations are used in the formulation of the problem. In the limit of shallow cavity, parallel flow approximation is adopted and the result established that the flow intensity, heat and mass transfer are considerably affected by radiation absorption and magnetic field depending on whether the vertical solutal gradient is stabilizing or destabilizing. A critical radiation value, depending on the thermal Rayleigh number, for the onset of unstable convection is also established in this study. The effect of Soret is also mentioned.

Copyright © 2015 Amos and Israel-Cookey. This is an open access article distributed under the Creative Commons Attribution License, which permits unrestricted use, distribution, and reproduction in any medium, provided the original work is properly cited.

Citation: Amos, E. and Israel-Cookey, C. 2015. "Magnetic and radiation absorption effects on thermosolutal convection in a horizontal porous layer subject to cross fluxes of heat and mass", *International Journal of Current Research*, 7, (7), 18328-18339.

INTRODUCTION

Combined heat and mass transfer on double diffusive convection in electrically conducting binary fluid is a subject of intense research due to the occurrence of such fluids in nuclear engineering heat transfer, industrial problems involving sudden heating or cooling, solute intrusion in sediments in coastal environments, chemical processes and specie transport through biological membranes and many others. Over the years, special reviews and documentation has been given to this area especially as shown in the works of Mamou *et al.* (2001), Mansour *et al.* (2008). Amahmid *et al.* (1999) studied double diffusive convection in a horizontally sparsely packed porous system subject to vertical fluxes of heat and solute using the Brinkman model and the threshold for the onset of subcritical and stationary convection were determined. Mamou and Vasseur (1999), Kalla *et al.* (2001) studied lateral heating on bifurcation phenomena present in double diffusive convection and found that the lateral heating acts as an imperfection brought to the bifurcation curves. Multiple steady state solutions with different heat and mass transfer rates were found to co-exist. Liu *et al.* (2008) studied double diffusive natural convection within a vertical porous enclosure with localized heating and salting from one side using the finite element based volume method. Their result showed that the heat and mass transfer rates can be controlled to a certain extent by varying the relative position of the heating elements. Kumar and Mohan (2012) studied double diffusive convection in an Oldroydian viscoelastic fluid under the simultaneous effects of magnetic field and suspended particles through a porous medium. Among the numerous studies devoted to modeling of the electromagnetic stabilization of convective flows in several configurations and at some fixed values of the governing parameters is that of Gelfgat and Bar-Yoseph (2001), Hassanien and Obied-Allah (2002) and Kaddeche *et al.* (2003), Cheng (1999), Rakoto-Ramambason and Vasseur (2007).

Sheikholeslam *et al.* (2014) showed MHD effect on natural convection heat transfer in an L-shaped enclosure filled with nanofluid. They showed the effect of Hartmann number, volume fraction of nanoparticles, Rayleigh number and inclination angle on streamline. Many engineering flow processes take place at high temperature and many of such fluids can be electrically conducting.

*Corresponding author: Amos, E.

Department of Mathematics and Computer Science, Rivers State University of Science and Technology, Port Harcourt, Nigeria.

Accordingly knowledge of radiative heat transfer and magnetic field become essential since both are correlative in many application fields (Ogulu and Amos, 2002). The process of cooling of the first wall inside a nuclear reactor containment vessel where the hot plasma is isolated from the wall by applying magnetic field is one example of such field. A numerical study of conjugated heat (natural convection-thermal radiation) and mass in a square cavity filled with a mixture of Air-CO₂ was studied by Serrano-Avellano and Gijon-Rivera (2014) and showed that radiative heat transfer does have effect on the flow especially for high Rayleigh number. According to reasonable simplification, many researchers studied the effects of radiation in convective flows. For optically thick fluids, where self-absorption exist, the Rosseland approximation was used to describe radiative heat flux in the energy equation (Azzam, 2002; Israel-Cookey and Amos, 2014).

In view of the above studies, it is therefore important to consider the simultaneous effect of radiative heat and magnetic field on flow structures alongside the imposition of cross fluxes of heat and mass.

Mathematical formulation

Assuming two-dimensional flow, double diffusive convection is studied in a horizontal porous layer of length L , height H , permeability K , and saturated with a binary fluid (see Figure 1). The origin of the coordinate system is located at the centre of the cavity with x', y' being the horizontal and vertical coordinates respectively. Heat flux hq' is applied on the horizontal walls while fluxes of heat q' and mass j' is applied on the horizontal walls. The porous medium is considered to be uniform and in local thermal and compositional equilibrium with the fluid. The effects due to viscous dissipation and porous medium inertial forces are assumed negligible.

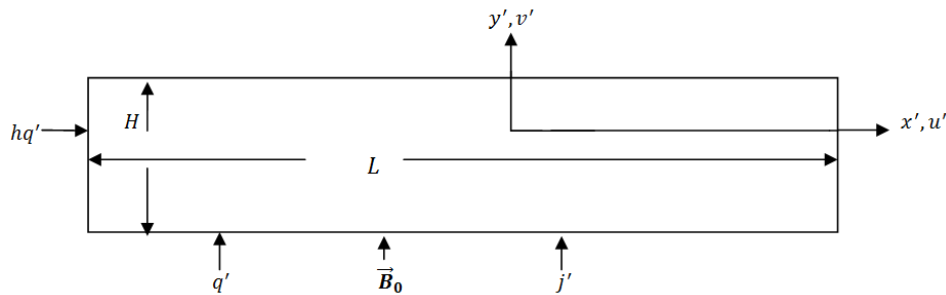


Figure 1. Schematic of the physical problem

The binary fluid is assumed to be Newtonian, radiating and incompressible. We also assume that the porous medium satisfies the Oberbeck-Boussinesq approximation, (Nield and Bejan, 2006),

$$\rho = \rho_0 [1 - \beta_T (T' - T_0) - \beta_c (C' - C_0)] \dots\dots\dots (1)$$

Where the subscript zero refers to reference state, β_T and β_c are thermal expansion coefficient and concentration expansion coefficient respectively and are evaluated at the reference state. A magnetic field of intensity \vec{B}_0 is applied perpendicular to the channel. Hence using the Darcy model and taking into account the Soret effect, the dimensional governing equation expressing continuity, momentum, energy and specie concentration are

$$\vec{\nabla}' \cdot \vec{V}' = 0 \dots\dots\dots (2)$$

$$\frac{\mu}{\kappa} \vec{V}' = -\vec{\nabla}' P' + \rho \vec{g} + j_e \times \vec{B}_0 \dots\dots\dots (3)$$

$$(\rho c)_p \frac{\partial T'}{\partial t'} + (\rho c)_f (\vec{V}' \cdot \vec{\nabla}' T') = \kappa \vec{\nabla}'^2 T' - \vec{\nabla}' \cdot q'_r \dots\dots\dots (4)$$

$$\epsilon' \frac{\partial C'}{\partial t'} + \vec{V}' \cdot \vec{\nabla}' C' = D \vec{\nabla}'^2 C' + D^* C'_0 \vec{\nabla}'^2 T' \dots\dots\dots (5)$$

where $(\rho c)_p$ and $(\rho c)_f$ are the heat capacity of the porous medium and the fluid respectively, κ , the permeability of the porous medium, \vec{V}' is the Darcy velocity, q'_r is the radiative flux, ϵ' is the porosity of the porous medium.

For optically thick fluids, where self-absorption exists, the Rosseland approximation (Israel-Cookey and Amos, 2014) is used to describe the radiative flux in the energy equation. That is

$$q'_r = - \frac{4\sigma^* \nabla T^4}{3\delta} \dots\dots\dots(6)$$

where σ^* is the Stephen - Boltzmann constant, δ is the mean absorption coefficient. We now assume that the temperature differences within the fluid and the porous medium is sufficiently small such that T^4 may be expressed as a linear function of temperature, T . By using Taylor's series expansion about the free stream temperature, T_o , and neglecting higher order term, we obtain

$$T'^4 \approx 4T_o^3 T' - 3T_o^4 \dots\dots\dots(7)$$

Consequently equation (4) becomes

$$(\rho c)_p \frac{\partial T'}{\partial t'} + (\rho c)_f (\vec{v}' \cdot \vec{\nabla} T') = \kappa \nabla'^2 T' + \frac{16\sigma^* T_o^3 \nabla'^2 T'}{3\delta} \dots\dots\dots (8)$$

We note that the electric current \vec{j}_e is defined by

$$\vec{j}_e = \sigma(-\vec{\nabla}\phi_e + \vec{v}' \times \vec{B}) \dots\dots\dots(9)$$

and

$$\vec{\nabla} \cdot \vec{j}_e = 0 \dots\dots\dots (10)$$

where σ is electrical conductivity and ϕ_e is the electric potential. Equation (9) is the Ohm's law and equation (10) is the conservation of electric current.

With electrically insulated boundaries, the electric potential ϕ_e is constant and in most laboratory experiments, the magnetic Reynolds number is very small (Kaddeche *et al.*, 2003) and the magnetic field remains almost unperturbed and having neglected the induced magnetic field, equation (3) becomes

$$\frac{\mu}{\kappa} \vec{v}' = - \vec{\nabla}' P' + \rho \vec{g} - \sigma \beta_o^2 \vec{v}' \dots\dots\dots(11)$$

Using Equation (1) on (11), eliminating the pressure in the resulting expression and employing the stream function formalism, we have

$$\nabla'^2 \psi' = - \frac{\bar{g} \beta_T K}{\nu} \left(\frac{\partial T'}{\partial x'} + \frac{\beta_c}{\beta_T} \frac{\partial C'}{\partial x'} \right) - \sigma \frac{B_o^2 K}{\mu} \nabla'^2 \psi' \dots\dots\dots (12)$$

where ψ' is the stream function and $u = \frac{\partial \psi'}{\partial y'}$, $v = -\frac{\partial \psi'}{\partial x'}$ such that equation (2) is satisfied.

Consequently, the governing equation are now equations (5), (8) and (12) and are to be solved subject to the boundary conditions:

$$\begin{aligned} \psi' = 0, \frac{\partial T'}{\partial x'} = -\frac{hq'}{k}, \frac{\partial C'}{\partial x'} = \frac{hD^* C'_o q'}{D\kappa} \quad \text{at } x' = \pm \frac{L}{2} \\ \psi' = 0, \frac{\partial T'}{\partial y'} = -\frac{hq'}{k}, \frac{\partial C'}{\partial y'} = -\frac{j}{D} + \frac{D^* C'_o q'}{Dk} \quad \text{at } y' = \pm \frac{H}{2} \end{aligned} \dots\dots\dots(13)$$

We now introduce the following non dimensional variables into equations (5), (8), (12) and (13),

$$\begin{aligned}
 (x, y) &= \frac{(x', y')}{H'}, \quad \vec{V}' = (u, v) = \frac{(u', v')}{\alpha} H', \quad t = \frac{t' \gamma}{\phi H'^2}, \quad \varepsilon = \frac{\varepsilon'}{\phi}, \quad \theta = \frac{T' - T_o}{\Delta T'} \\
 C &= \frac{C' - C_0}{\Delta C'}, \quad \psi = \frac{\psi'}{\alpha}, \quad \Delta T' = \frac{q' H'}{\kappa}, \quad \Delta C' = \frac{j H'}{D}, \quad Le = \frac{\alpha}{D} \dots\dots\dots(14) \\
 R_T &= \frac{\bar{g} \beta_T K q' H'^2}{\kappa \nu \alpha}, \quad R_C = \frac{\bar{g} \beta_C K j H'^2}{\nu D^2}, \quad R = \frac{16 \sigma^* T_o^3}{3 \kappa \delta}, \quad \alpha = \frac{k}{(\rho c)_f}
 \end{aligned}$$

where $\phi = \frac{(\rho c)_p}{(\rho c)_f}$ is the heat capacity ratio.

The result is

$$(1 + M^2) \nabla^2 \psi = - \left(R_T \frac{\partial \theta}{\partial x} + \frac{R_C}{Le} \frac{\partial C}{\partial x} \right) \dots\dots\dots(15)$$

$$\frac{\partial \theta}{\partial t} + u \frac{\partial \theta}{\partial x} + v \frac{\partial \theta}{\partial y} = (1 + R^2) \nabla^2 \theta \dots\dots\dots(16)$$

$$\varepsilon \frac{\partial C}{\partial t} + u \frac{\partial C}{\partial x} + v \frac{\partial C}{\partial y} = \frac{1}{Le} [\nabla^2 C + S \nabla^2 \theta] \dots\dots\dots(17)$$

The corresponding boundary conditions are

$$\psi = 0, \frac{\partial \theta}{\partial x'} = -h, \frac{\partial C}{\partial x} = hS \quad \text{for } x = \pm \frac{A_r}{2} \dots\dots\dots(18)$$

$$\psi = 0, \frac{\partial \theta}{\partial y} = -1, \frac{\partial C}{\partial y} = -1 + S \quad \text{for } y = \pm \frac{1}{2}$$

where $A_r = \frac{L'}{H'}$ is the cavity aspect ratio.

The thermal Rayleigh number R_T and the solutal Rayleigh number R_C are related by

$$R_C = R_T N Le \quad \text{where} \quad N = \frac{\beta_C}{\beta_T} \frac{\Delta C'}{\Delta T'} \dots\dots\dots(19)$$

The heat and mass transfer rates are expressed in term of the Nusselt and Sherwood numbers respectively as

$$Nu = \frac{1}{\Delta \theta} \quad \text{and} \quad Sh = \frac{1}{\Delta C} \dots\dots\dots(20)$$

METHOD OF SOLUTION

In general, analytical solutions to equations (15) – (18) is difficult to obtain. However, in the limit of shallow cavity ($A_r \gg 1$), it is possible to find approximate solutions (Bahloul *et al.* (2003) and hence using the parallel flow approximation we have the following simplifications:

$$\psi(x, y) = \psi(y), \quad \theta(x, y) = S_\theta x + \phi_\theta(y), \dots\dots\dots(21)$$

$$C(x, y) = S_c x + \phi_c (y)$$

Using equation (21) in equations (15) – (18) we obtain

$$(1 + M^2) \frac{d^2 \psi}{dy^2} = -R_T (S_\theta + N S_C) \dots\dots\dots(22)$$

$$(1 + R^2) \frac{d^2 \phi_\theta}{dy^2} = S_\theta \frac{d\psi}{dy} \dots\dots\dots(23)$$

$$S \frac{d^2 \phi_\theta}{dy^2} + \frac{d^2 \phi_C}{dy^2} = Le S_C \frac{d\psi}{dy} \dots\dots\dots(24)$$

Subject to the boundary conditions in the *y* direction

$$\psi = 0, \frac{d\phi_\theta}{dy} = -1, \frac{d\phi_C}{dy} = -1 + S \text{ at } y = \pm \frac{1}{2} \dots\dots\dots (25)$$

where S_θ and S_C are constants.

The solutions of equations (22) – (24) using (25) are

$$\psi = \psi_0 (1 - 4y^2) \dots\dots\dots (26)$$

$$\theta(x, y) = S_\theta x - y + \frac{\psi_0 S_\theta}{3(1 + R^2)} (3y - 4y^3) \dots\dots\dots(27)$$

$$C(x, y) = S_C x + (S - 1)y + \frac{\psi_0}{3} (Le S_C - \frac{SS_\theta}{1 + R^2}) (3y - 4y^3) \dots\dots\dots(28)$$

$$\text{where } \psi_0 = \frac{R_T}{8(1 + M^2)} (S_\theta + N S_C) \dots\dots\dots(29)$$

is the value of the stream function at the centre of the enclosure. The equations for the constants S_θ and S_C are based on heat and solute balances across any transversal section of the cavity.

$$\text{Thus } \int_{-\frac{1}{2}}^{\frac{1}{2}} \left[u \theta - (1 + R^2) \frac{\partial \theta}{\partial x} \right] dy = h \dots\dots\dots(30)$$

and

$$\int_{-\frac{1}{2}}^{\frac{1}{2}} \left[u C - \frac{1}{Le} \left(\frac{\partial C}{\partial x} + S \frac{\partial \theta}{\partial x} \right) \right] dy = 0 \dots\dots\dots (31)$$

On evaluation of (30) and (31) we obtain

$$S_\theta = \frac{(10\psi_0 - 15h)(1 + R^2)}{8\psi_0^2 + 15(1 + R^2)^2} \dots\dots\dots(32)$$

and

$$S_C = \frac{8Le SS_\theta \psi_0^2 - 15(1 + R^2) SS_\theta - 10Le(S - 1)(1 + R^2)\psi_0}{(1 + R^2)(8\psi_0^2 Le^2 + 15)} \dots\dots\dots (33)$$

Substituting equations (32) and (33) into equation (29) yields,

$$\psi_0^5 + A\psi_0^3 + B\psi_0^2 + C\psi_0 + D = 0 \tag{34}$$

where

$$A = 80d [12(1 + M^2)\{(1 + R^2)^2 Le^2 + 1\} - R_T Le \{(1 + R^2) Le - NS - N(S - 1)\}]$$

$$B = 120d R_T Le h [(1 + R^2) Le + NS]$$

$$C = -150d [R_T (1 + R^2) \{(1 + NS) - Le(S - 1)(1 + R^2)\} - 12(1 + M^2)(1 + R^2)^2]$$

$$D = 225 R_T dh (1 + R^2) (1 - NS)$$

$$d = \frac{1}{512 Le^2 (1 + M^2)}$$

For given values of R_T, Le, N, R, h, S , equation (34), is solved numerically.

The heat and mass transfer are given according to (20), that is

$$Nu = \frac{1}{\Delta\theta} = \frac{1}{[\theta(0, -\frac{1}{2}) - \theta(0, \frac{1}{2})]}$$

$$= \frac{3(1 + R^2)}{3(1 + R^2) - 2\psi_0 S_\theta} \tag{35}$$

$$Sh = \frac{1}{\Delta C} = \frac{1}{[C(0, -\frac{1}{2}) - C(0, \frac{1}{2})]}$$

$$= -\frac{3(1 + R^2)}{3(S - 1)(1 + R^2) + 2\psi_0 [Le S_c (1 + R^2) - S S_\theta]} \tag{36}$$

Setting $\psi_0 = 0$, the purely diffusive state is obtained from equation (27) and (28), that is,

$$\theta(x, y) = \frac{-hx}{1 + R^2} - y \tag{37}$$

$$C(x, y) = \frac{hSx}{1 + R^2} + (S - 1)y \tag{38}$$

Thus for the purely diffusive state the heat and mass transfer is

$$Nu = 1 \tag{39}$$

and

$$Sh = \frac{1}{1 - S} \tag{40}$$

RESULTS AND DISCUSSION

Convective motion induced by a combination of thermal and solutal buoyancy forces arising from thermal and solutal boundary conditions applied on the enclosure are obtained under parallel flow approximation and numerically using the software

‘mathematica’ (Wolfram, 1991), to solve equation (34) with given values of $R_T, Le, \nu, \alpha, \mu$ and S . Up to five solutions are possible but we consider only the ones that are real. The evolution of the flow intensity, $|\Psi_0|$, the heat and mass transfer, Nu and Sh respectively and the possibility of any unstable branch depends on the values attributed to the governing parameters. In general, both the intensity and direction of rotation of the convective flow within the porous layer are strongly affected by the buoyancy ratio, N , the Soret, S , the magnetic parameter, M , the radiation parameter, R , the lateral heating parameter, h , and the thermal Raleigh number, R_T . Points in the tables with ‘-’ indicates entry which otherwise would have been a complex value.

SOLUTAL DOMINATED AIDING FLOW

For $N > 0$, we have typical features of aiding thermal and solutal forces. Three real solutions for the stream function are obtainable in this case and are denoted by $\Psi_{0,1}$ (clockwise), $\Psi_{0,2}$ and $\Psi_{0,5}$ (counterclockwise). Table 1 shows that as the radiation parameter, R , is increased, an initially stable $\Psi_{0,1}$ solution for the stream function becomes unstable at the critical radiation value of $R_{cr} = 2.01$ when $R_T = 10$. This critical radiation value depends on the thermal Rayleigh number. Increase in the thermal Rayleigh number increases the critical radiation value. This critical radiation value is unaffected by change in Soret. One of the counterclockwise branches, $\Psi_{0,2}$ exhibited weak flow and was aided to be at rest by increasing Soret, specifically at $S \geq 0.5$, and this is irrespective of increase or decrease in the thermal Raleigh number.

Table 1. Influence of Soret and radiation on the flow intensity for $Le = 10, N = 2, h = 0.2, R_T = 10$

S	R	$\Psi_{0,1}$	$\Psi_{0,2}$	$\Psi_{0,5}$
0	0.1	-3.37867	0.0144294	3.09891
	0.3	-3.46192	0.0133985	3.17487
	0.5	-3.61298	0.0117257	3.31178
	2.0	-3.89287	0.00299956	3.13768
	2.1	-3.87426	0.00297591	3.11577
	5.0	-1.61925	0.000581265	1.54148
0.5	0.1	-3.3651	0	3.04591
	0.3	-3.44582	0	3.11991
	0.5	-3.59192	0	3.2524
	2.0	-3.59472	0	2.51135
	2.1	-3.56942	0	2.47803
	5.0	-1.151	0	1.07332

Figure 2a shows that, though, increase in radiation decreases heat transfer by convection, the heat transfer inside the cavity is increased by the thermal Rayleigh number. Increase in radiation absorption also decreases mass transfer, (figure 2b). The effect of the thermal Rayleigh number is not as significant since at $R_T \geq 32$ the mass transfer rates for $R = 2$ and $R = 0.3$ are the same. Also for all the displayed values of R , the mass transfer rates are nearly the same at $R_T \geq 68$.

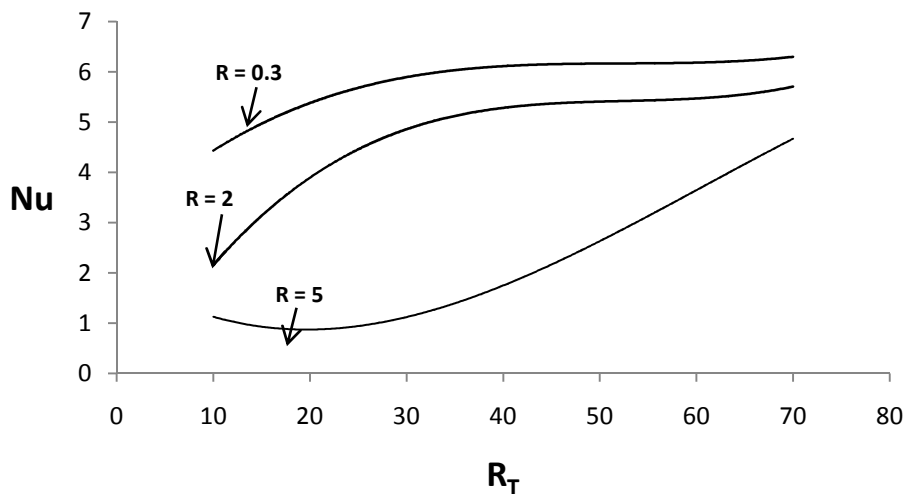


Figure 2a: Influence of radiation and thermal Rayleigh number on heat transfer for $S = 0.5, M = 0.5, Le = 10, N = 2, h = 0.2$

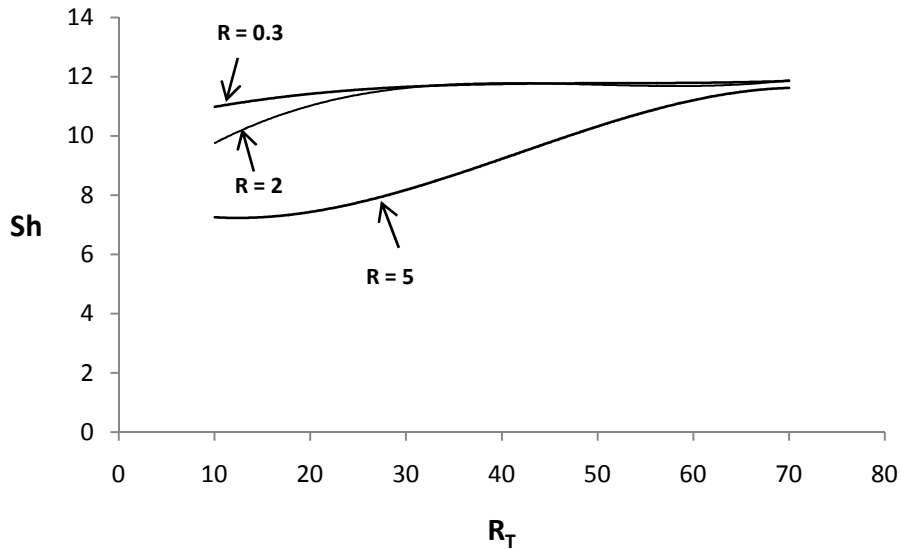


Figure 2b: Influence of radiation and thermal Rayleigh number on mass transfer for $S = 0.5$, $M = 0.5$, $Le = 10$, $N = 2$, $h = 0.2$

Table 2 shows that the flow intensity decreases with increase in magnetic field. The counterclockwise branch, $\Psi_{0,2}$, remains near the rest state as the Soret is increased and perfectly at rest when $S \geq 0.5$. Figure 3 indicates that for a given thermal Rayleigh number, R_T , the flow is considerably inhibited by the retarding effect of the electromagnetic body force. The thermal Rayleigh number itself increases the flow intensity

Table 2. Influence of Soret and magnetic field on the flow intensity for $R_T = 10$, $R = 0.5$, $Le = 10$, $N = 2$ and $h = 0.2$

S	M	$\Psi_{0,1}$	$\Psi_{0,2}$	$\Psi_{0,5}$
0	0	-4.09551	0.011704	3.80332
	0.5	-3.61298	0.0117257	3.31178
	1	-2.73415	0.0117915	2.40527
	2	-1.43263	0.0120622	1.04947
	5	-0.362267	0.0143861	0.27513
	7	-0.218683	0.0150275	0.165163
	0.5	0	-4.07856	0
0.5		-3.59192	0	3.2524
1		-2.70088	0	2.31339
2		-1.34364	0	0.739301
5		-0.239634	0	0.156179
7		-0.105692	0	0.0667733

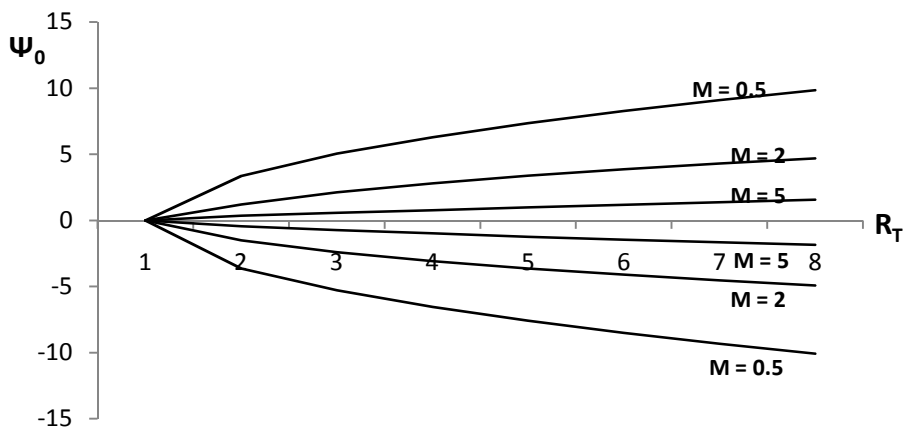


Figure 3. Influence of thermal Rayleigh number and magnetic field on the flow intensity for $Le = 2$, $h = 0.2$, $S = -0.5$, $N = 2$ and $R = 0.5$

Table 3 shows that the flow circulation and transfer are decreased by the magnetic field. Consequently at $M = 5$ the heat transfer is almost by pure conduction ($N \approx 1$). The mass transfer shows significant change in Soret but not in magnetic field. For $M < 2$, Sh is rather related to concentration distribution within the cavity induced by the Soret effect and by convection, with decrease in mass transfer when $M \geq 2$ and $S \geq 0$.

Table 3. Influence of Soret and magnetic field on Heat and mass transfer for $R_T = 20, R = 0.5, Le = 10, N = 2$ and $h = 0.2$

S	M	$\Psi_{0,1}$	Nu	Sh
0	0	-5.94222	5.58396	5.98412
	0.5	-5.28271	5.33124	5.97992
	1	-4.09551	4.64522	5.96669
	2	-2.37201	2.96456	5.90199
	5	-0.627893	1.21555	4.88998
0.5	0	-5.93410	5.58128	11.5602
	0.5	-5.27226	5.32661	11.4534
	1	-4.07856	4.63277	11.1406
	2	-2.33028	2.91573	9.99721
	5	-0.481625	1.13869	5.68253

Heat transfer driven flows

For the particular case $N = 0$, the solutal buoyancy forces are null and the flow intensity induced by radiative flux and the thermal fluxes imposed on the vertical walls of the cavity increases. Three convective solution are possible one clockwise, $\Psi_{0,1}$, and two counterclockwise, $\Psi_{0,4}$ and $\Psi_{0,5}$, (but two are shown in Table 4). The clockwise branch becomes unstable at the critical radiation value $R_{cr} = 3.1$. It is observed that the cross fluxes of heat aid the clockwise motion but oppose the counterclockwise motion. At $R = 3.8$ and $h = 0.1$ only one convective solution is possible. Increasing the cross fluxes to $h = 0.2$ reduces the radiation value to $R = 3.7$ for one convective solution to persist.

Table 4. Influence of radiation and lateral heating on the stream function for $R_T = 30, M = 0.5, Le = 10, N = 0, S = 0.5$

h	R	$\Psi_{0,1}$	$\Psi_{0,5}$
0.1	0	-0.538156	5.22141
	0.5	-5.95938	5.79654
	2	-10.2624	10.0441
	3	-10.8012	10.4006
	3.1	-10.5709	10.1248
	3.2	-10.259	9.75352
	3.5	-8.67158	7.78878
	3.7	-6.77092	4.68864
	3.8	-5.39838	--
	4	-2.10668	--
0.2	0	-5.45659	5.13541
	0.5	-6.03607	5.70964
	2	-103666	9.9294
	3	-10.986	10.1814
	3.1	-10.7745	9.87723
	3.2	-10.4864	9.46741
	3.5	-9.02925	7.1932
	3.6	-8.28068	5.54382
	3.7	-7.35277	--
	4	-3.47899	--
5	-0.479773	--	

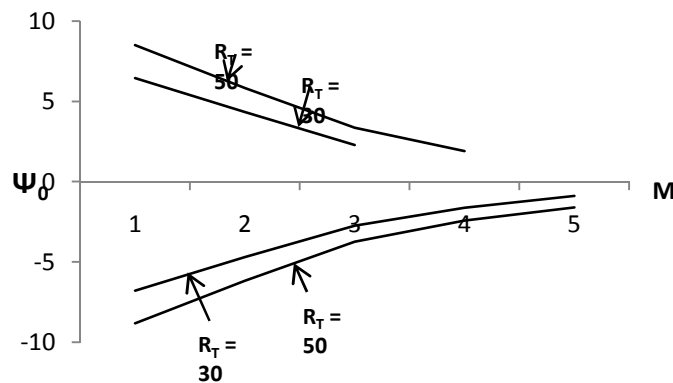


Figure 4. Influence of magnetic field and thermal Rayleigh number on the flow intensity for $R = 0.5, S = -0.5, Le = 10, h = 0.2$ and $N = 0$

Figure 4 shows that increasing the magnetic field, M , decreases the flow intensity and this trend remains even on increase or decrease in Soret, while increasing the thermal Rayleigh number, R_T increases the flow intensity for both clockwise and counterclockwise motions. The retarding effect of the magnetic field is such that for the clockwise branch at $M > 3$, $R_T=30$ and $M > 4$, $R_T = 50$ respectively, no convective solution is observed. Similarly for the counterclockwise branch, at $M > 4$, $R_T > 50$ no convective solution is observed. The other counterclockwise solution, $(\Psi_{0,4})$, remains near the rest state and is almost unchanged with increasing R_T (although not shown in our representations).

Solutal dominated opposing flow

The typical feature of opposing double diffusive flow ($N<0$) is considered with the main contribution for buoyancy due to the solutal one. Up to five solutions are possible for the stream function depending on the values attributed to the governing parameters. Because of the peculiarities of the characteristics exhibited by these solution, the stream function value will still be denoted by $\Psi_{0,1}$, $\Psi_{0,2}$, $\Psi_{0,3}$, $\Psi_{0,4}$ and $\Psi_{0,5}$. These solution are either clockwise, counterclockwise or of the rest state.

Table 5 provides exemplary result under the influence of radiation, Soret and thermal Rayleigh number. Two clockwise, two counterclockwise and a rest state solution prevails at $S = -0.5$. At $S = -0.25$, the rest state disappears and becomes convective (clockwise) though of low intensity and remains so even at $S = 0.5$. A stability analysis of $\Psi_{0,1}$ shows that it is unstable at the critical radiation value $R_{cr}=2.7$. This critical radiation value is unaffected by Soret at the same thermal Rayleigh number. The counterclockwise solution increases in intensity as the radiative flux is increased and has no real value at certain radiation values depending on the thermal Rayleigh number.

Table 5. Influence of radiation and Soret on the stream function for $Le = 10, N = -2, h = 0.2$ and $M = 0.5, R_T = 30$

S	R	$\Psi_{0,1}$	$\Psi_{0,2}$	$\Psi_{0,3}$	$\Psi_{0,4}$	$\Psi_{0,5}$
-0.5	0	-4.84043	-0.684383	0	1.17298	4.35183
	0.5	-5.46717	-0.778987	0	1.23905	5.00711
	2	-9.87001	-1.89489	0	1.23905	9.34643
	2.6	-10.5564	-2.78211	0	3.53773	9.80073
	2.7	-10.5114	-2.28798	0	3.82449	9.67488
	3	-9.92313	-3.82425	0	5.2451	8.51287
	3.1	-9.50078	-4.23788	0	--	--
	3.2	-8.86796	-4.80834	0	--	--
	3.3	-7.70177	-5.85257	0	--	--
	3.4	--	--	0	--	--
0.5	0	-4.85642	-0.233179	-0.0944631	0.704286	4.47978
	0.5	-5.49467	-0.315626	-0.0632616	0.705099	5.12296
	2	-10.0079	-0.973871	-0.012471	1.45548	9.53875
	2.6	-10.8355	-1.43789	-0.00789904	2.08763	10.1937
	2.7	-10.8349	-1.54003	-0.00738006	2.2402	10.1421
	3	-10.485	-1.92638	-0.00608965	2.87567	9.54182
	3.4	-8.73623	-2.88249	-0.00482672	--	--
	3.5	-7.84112	-3.37017	-0.00457124	--	--
	3.7	--	--	-0.00411656	--	--

Table 6 shows, as usual, the inhibiting action of the magnetic field for both clockwise and counterclockwise motions. The thermal Rayleigh number greatly enhances the flow intensity. The heat transfer decreases for increase in magnetic field in the counterclockwise motion in much more appreciable rate than that of clockwise motion. At $M \geq 2$, depending on the thermal Rayleigh number, no real solution exist for the stream function for the $\Psi_{0,5}$ branch. Our numerical computations show that the asymptotic branch, $\Psi_{0,3}$, of the flow induce nearly a constant heat and mass transfer rate for all thermal Rayleigh number, R_T examined and when $N = -2$, the purely diffusive state ($Nu = 1$ and $Sh = 0.666667$) is achieved.

Table 6. Influence of magnetic field and thermal Rayleigh number on the stream function and Heat and mass transfer for $Le = 10, N = -1, R = 0.5$, and $h = 0.2$

R_T	M	$S = 0.5$			$S = 0.5$		
		$\Psi_{0,1}$	Nu	Sh	$\Psi_{0,5}$	Nu	Sh
10	0	-3.54727	4.19988	10.19988	3.13701	2.55542	10.8768
	0.5	-3.09767	3.76802	10.6591	2.64969	2.24231	10.5928
	2	-0.769	1.30446	6.91718	--	--	--
	5	-0.047985	1.00597	2.04046	--	--	--
20	0	-5.23628	5.31049	11.4466	4.8823	3.47355	11.4366
	0.5	-4.63685	5.00094	11.312	4.27057	3.19043	11.2968
	2	-1.89448	2.40359	9.43538	--	--	--
	5	-0.0690419	1.00912	2.15425	--	--	--
50	0	-8.45521	6.07938	11.7756	8.12716	4.44582	11.7735
	0.5	-7.53932	5.05874	11.7202	7.20725	4.24028	11.7172
	2	-3.54727	4.19988	10.9164	3.13701	2.55542	10.8768
	5	-0.68601	1.25045	6.61823	--	--	--

Conclusion

Natural convection of a binary fluid saturating a horizontal porous medium under the influence of radiation and magnetic field is investigated and their effect on the strength of the convection $|\Psi_0|$, the heat transfer, Nu , and mass transfer, Sh , are predicted using the parallel flow approximation technique and discussed accordingly. Consequently in the presence of cross fluxes of heat and mass, we make the following remarks:

- (i) For positive values of, N when the vertical solutal gradient is stabilizing the flow pattern is characterized by the existence of clockwise and counterclockwise convection which depends strongly on the magnitude of R_T , N and S . For relatively low values of R_T , the intensity of the flow pattern decreases. Upon increasing R_T the flow intensity increases. The critical radiation, R_{cr} , value for unstable convection depends on R_T . The flow intensity is generally inhibited by the electromagnetic force.
- (ii) In the case for pure thermal convection, increasing the thermal Rayleigh number increases the flow intensity, while increase in the magnetic field decreases the flow intensity. The cross fluxes aid the clockwise motion but decrease the counterclockwise motion. Increasing the vertical gradient of heat enhances flow intensity.
- (iii) For negative values of N , the vertical solutal gradient is destabilizing. Increasing the vertical gradient of heat increases the flow intensity. Increased magnetic field decreases the flow intensity and rate of heat transfer but enhances mass transfer. Both clockwise and counterclockwise flow intensity induce, nearly, the same rate of mass transfer under the action of magnetic field. The asymptotic branch of the flow intensity induce nearly a constant heat and mass transfer for all thermal Rayleigh number, R_T and when $N = -2$, the purely diffuse state is achieved. Again the critical radiation R_{cr} value for unstable flow as determined in this study depends on the thermal Rayleigh number, R_T .

While the result presented here were obtained for a rather idealized geometry, we expect our qualitative findings to be more widely applicable. From a particular point of view, the key implication of our result is that when simulating geothermal system where the onset of convection may substantially increase the heat flux in the system, our result suggest that magnetic stabilization on the process could be very important. Consistent with the observation of Trevesan and Bejan (1986), Liu *et al* (2008) we note, in general, that the average Nusselt number are less in the opposing flow area than for the corresponding aiding flow range due to the fact that the opposing flow has a lower rate adjacent to the sink than the corresponding aiding flow case.

REFERENCES

- Amahmid, A., Hasnaoui, M., Mamou, A. and Vasseur, P. 1999. Double-diffusive parallel flow induced in a horizontal Brinkman porous layer subjected to constant heat and mass fluxes: Analytical and Numerical Studies. *Heat and mass Transfer*, 35, 409-421.
- Azzam, G. E. A. 2002. Radiation effects on the MHD mixed free-forced convective flow past a semi-infinite moving vertical plate for high temperature difference. *Physica Scripta*, 66, 71-76.
- Bahloul, A., Boutana, N., Vasseur, P. 2003. Double-diffusive and Soret-induced convection in a shallow horizontal porous layer. *Journal of Fluid Mechanics*, 491, 325-352.
- Cheng, C. Y. 1999. Effect of magnetic field on heat and mass transfer by natural convection from vertical surfaces in a porous media- an integral approach. *International Communications of Heat and Mass Transfer*, 26, 935-943.
- Gelfgat, A.Y. and Bar-Yoseph, P.Z. 2001. The Effect of an external Magnetic field on oscillatory instability on convective flows in a rectangular cavity. *Physics of Fluids*, 13(8), 2269-2278.
- Hassanien, I. A. and Obied Allah, M.H. 2002. Oscillatory hydromagnetic flow through a porous medium with variable permeability in the presence of free convection and mass transfer flow. *International Communicational of Heat and Mass Transfer*, 29, 567-575.
- Israel-Cooke, C. and Amos, E. 2014. Soret and radiation absorption effects on the onset of magneto-thermosolutal convection in a porous medium. *Journal of Applied Mathematics and and Bioinformatics*, 4(1), 71-87.
- Kaddeche, S., Henry, D. and Benhadid, H. 2003. Magnetic stabilization of the buoyant convection between infinite horizontal walls with a horizontal temperature gradient. *Journal of Fluid Mechanics*, 480, 185-216.
- Kalla, L., Mamou, M., Vasseur, P. and Robillard, L. 2001. Multiple solution for double-diffusive convection in a shallow porous cavity with vertical fluxes of heat and mass. *International Journal of Heat and Mass Transfer*, 44, 4493-4504.
- Kumar, P. and Mohan, H. 2012. Double-diffusive convection in a viscoelastic fluid. *Tamkang Journal of Mathematics*, 43(3), 365-374.
- Liu, D., Zhao, F. Y. and Tang, G. F. 2008. Thermosolutal convection in saturated porous enclosure with concentration energy and solute sources. *Energy Conservation Management*, 49, 16-31.
- Mamou, M. and Vasseur, P. 1999. Thermosolutal bifurcation phenomena in porous enclosure subjected to vertical temperature and concentration gradient. *Journal of Fluid Mechanics*, 395, 61-87.
- Mamou, M., Vasseur, P. and Hasnaoui, M. 2001. On numerical stability analysis of double-diffusive convection in confined enclosures. *Journal of Fluid Mechanics*, 433, 209-250.
- Mansour, A., Amahmid, A. and Hasnaoui, M. 2008. Soret Effect on Thermosolutal convection Developed in a Horizontal shallow porous layer salted from below and subject to cross fluxes of Heat. *International Journal of Heat and Fluid Flow*, 29, 306-314.
- Nield, D. A. and Bejan, A. 2006. *Convection in Porous Media*(3rd Ed). USA: Springer Publication.

- Ogulu, A. and Amos, E. 2002. Magnetohydrodynamic slip flow of a heat generating fluid with Hall currents. *AMSE. Mod. Meas. Cont. B*, 7(4), 51-57.
- Rakoto-Ramambason, D. S. and Vasseur, P. 2007. Influence of a magnetic field on natural convection in a shallow porous enclosure saturated with a binary fluid. *Acta Mechanica*, 191, 21-35.
- Serrano-Avelano, J. and Gijon-Rivera, M. 2014. Conjugate heat and mass transfer by natural convection in a square cavity filled with a mixture of Air-CO₂. *International Journal of Heat and Mass Transfer*, 70, 103-113.
- Sheikholeslam, M., Ganji, D.D., Gorji-Bandpy, M. and Soleimani, S. 2014. Magnetic field effect on nanofluid flow and heat transfer using KKL model. *Journal of the Taiwan Institute of Chemical Engineers*, vol 45, issue 3, 795-807.
- Trevesan, O.V. and Bejan, A. 1986. Mass and heat transfer by natural convection in a vertical slot filled with porous medium. *International Journal of Heat and Mass Transfer*, 29, 403-415.
- Wolfram, S. 1991. *Mathematica: A system of doing mathematics by computers*. England: Addison-Wesley Publishing.
